Computational Capabilities of Random Automata Networks for Reservoir Computing

David Snyder[1], Alireza Goudarzi[2], Christof Teuscher[1]

[1]*Portland State University, 1900 SW 4th Avenue,*
Portland, OR 97206 USA
[2]*University of New Mexico,*
1 University Boulevard Northeast Albuquerque, NM 87131 USA

This paper underscores the conjecture that intrinsic computation is maximal in systems at the "edge of chaos." We study the relationship between dynamics and computational capability in Random Boolean Networks (RBN) for Reservoir Computing (RC). RC is a computational paradigm in which a trained readout layer interprets the dynamics of an excitable component (called the reservoir) that is perturbed by external input. The reservoir is often implemented as a homogeneous recurrent neural network, but there has been little investigation into the properties of reservoirs that are discrete and heterogeneous. Random Boolean networks are generic and heterogeneous dynamical systems and here we use them as the reservoir. An RBN is typically a closed system; to use it as a reservoir we extend it with an input layer. As a consequence of perturbation, the RBN does not necessarily fall into an attractor. Computational capability in RC arises from a trade-off between separability and fading memory of inputs. We find the balance of these properties predictive of classification power and optimal at critical connectivity. These results are relevant to the construction of devices which exploit the intrinsic dynamics of complex heterogeneous systems, such as biomolecular substrates.

I. INTRODUCTION

Reservoir computing is an emerging paradigm that promotes computing using the intrinsic dynamics of an excitable system called the reservoir [1]. The reservoir acts as a temporal kernel function, projecting the input stream into a higher dimensional space, thereby creating features for the readout layer. To produce the desired output, the readout layer performs a dimensionality reduction on the traces of the input signal in the reservoir. Two advantages of RC are: computationally inexpensive training and flexibility in reservoir implementation. The latter is particularly important for systems that cannot be designed in a top-down way by traditional engineering methods. RC permits computation with physical systems that show extreme variation, interact in partially or entirely unknown ways, allow for limited functional control, and have a dynamic behavior beyond simple switching. This makes RC suitable for emerging unconventional computing paradigms, such as computing with physical phenomena [2] and self-assembled electronic architectures [3]. The technological promise of harnessing intrinsic computation with RC beyond the digital realm has enormous potential for cheaper, faster, more robust, and more energy-efficient information processing technology.

Maass et al. [4] initially proposed a version of RC called Liquid State Machine (LSM) as a model of cortical microcircuits. Independently, Jaeger [5] introduced a variation of RC called Echo State Network (ESN) as an alternative recurrent neural network approach for control tasks. Variations of both LSM and ESN have been proposed for many different machine learning and system control tasks (Lukosevicius and Jaeger [1]). Insofar, most of the

RC research is focused on reservoirs with homogeneous in-degrees and transfer functions. However, due to high design variation and the lack of control over these devices, most self-assembled systems are heterogeneous in their connectivity and transfer functions.

Since RC can be used to harness the intrinsic computational capabilities of physical systems, our study is motivated by three fundamental questions about heterogeneous reservoirs:

1. What is the relationship between the dynamical properties of a heterogeneous system and its computational capability as a reservoir?

2. How much does a reservoir need to be perturbed to adequately distribute the input signal? It may be infeasible to perturb the entire system. Also, a single-point perturbation may not propagate throughout the system due to its internal topology. Thus, we consider the size of the perturbation necessary to adequately distribute the input signal.

3. In a physical RC device, it may be difficult to observe the entire system. How much of the system and which components ought to be observed to extract features about the input stream?

We model the reservoirs with Random Boolean Networks (RBN), which are chosen due to their heterogeneity, simplicity, and generality. Kauffman [6] first introduced this model to study gene regulatory networks. He showed these Boolean networks to be in a complex dynamical phase at "the edge of chaos" when the average connectivity (in-degree) of the network is $\langle K \rangle = 2$ (critical connectivity). Rohlf et al. [7] showed that with near-critical connectivity information propagation in Boolean

networks becomes independent of system size. Packard [8] used an evolutionary algorithm to evolve Cellular Automata (CA) for solving computational tasks. He found the first evidence that connects critical dynamics and optimal computation in CA. Detailed analysis by Mitchell et al. [9] refuted this idea and accounted genetic drift, not the CA dynamics, for the evolutionary behavior of the CA. Goudarzi et al. [10] studied adaptive computation and task solving in Boolean networks and found that learning drives the network to the critical connectivity $\langle K_c \rangle = 2$.

Snyder et al. [11] introduced RBNs for RC, and found optimal task solving in networks with $\langle K \rangle > \langle K_c \rangle$. Here, using a less restrictive RC architecture, we find that RBNs with critical dynamics provided by $\langle K_c \rangle$ tend to offer higher computational capability than those with ordered or chaotic dynamics.

To be suitable for computation, a reservoir needs to eventually forget past perturbations, while possessing dynamics which respond in different ways due to different input streams. The first requirement is captured by *fading memory*. The *separation property* captures the second requirement and computes a distance measurement between the states of two identical reservoirs after being perturbed by two distinct input streams. It has been hypothesized that computational capabilities are optimal when the *separation property* is highest, but old input is eventually forgotten by the reservoir, which occurs when *fading memory* is lowest [12]. We extend the measurements described in [12, 13] to predict the computational capability of a reservoir in finite time-scales with a short-term memory requirement.

II. MODEL

A Reservoir Computing device is made up of three parts: input layer, reservoir, and readout layer [cf. Fig. 1]. The input layer excites the reservoir by passing an input signal to it, and the readout layer interprets the traces of the input signal in the reservoir dynamics to compute the desired output. In our model, the reservoir is a Random Boolean Network (RBN). The fundamental subunit of an RBN is a node with K input connections. At any instant in time, the node can assume either of the two binary states, "0" or "1." The node updates its state at time t according to a K-to-1 Boolean mapping of its K inputs. Therefore, the state of a single node at time $t + 1$ is completely determined by its K inputs at time t and by one of the 2^{2^K} Boolean functions used by the node. An RBN is a collection of N such binary nodes. For each node i out of N nodes, the node receives K_i inputs, each of which is connected to one of the N nodes in the network. In this model, self-connections are allowed.

The network is random in two different ways: 1) the source nodes for an input are chosen from the N nodes in the network with uniform probability and 2) the Boolean function of node i is chosen from the

$2^{2^{K_i}}$ possibilities with uniform probability. Each node sends the same value on all of its output connections to the destination nodes. The average connectivity will be $\langle K \rangle = \frac{1}{N} \sum_{i=1}^{N} K_i$. We study the properties of RBNs characterized by N nodes and average connectivity $\langle K \rangle$. This refers to all the instantiations of such RBNs. Once the network is instantiated, the collective time evolution at time t can be described as using $x_i^{t+1} = f_i(x_1^t, x_2^t, \ldots, x_{K_i}^t)$, where x_i^t is the state of the node i at time t and f_i is the Boolean function that governs the state update of the node i. The nodes are updated synchronously, i.e., all the nodes update their state according to a single global clock signal.

From a graph-theoretical perspective, an RBN is a directed graph with N vertices and $E = \langle K \rangle N$ directed edges. We construct the graph according to the random graph model [14]. We call this model a heterogeneous RBN because each node has a different in-degree. In the classical RBN model, all the nodes have identical in-degrees and therefore are homogeneous. The original model of Kauffman [6] assumes a static environment and therefore does not include exogenous inputs to the network. To use RBNs as the reservoir, we introduced I additional input nodes that each distribute the input signals to L randomly picked nodes in the network. The source nodes of K_i links for each node i are randomly picked from N nodes with uniform probability. The input nodes are not counted in calculating $\langle K \rangle$. For online computation, the reservoir is extended by a separate readout layer with O nodes. Each node in the readout layer is connected to each node in the reservoir. The output of node o in the readout layer at time t is denoted by y_o^t and is computed according to $y_o^t = sign\left(\sum_{j=1}^{N} \alpha_j x_j^t + b\right)$. Parameters α_j are the weights on the inputs from node j in the reservoir to node o in the readout layer, and b is the common bias for all the readout nodes. Parameters α_j and b can be trained using any regression algorithm to compute a target output [5]. In this paper, we are concerned with RBN-RC devices with a single input node, and a single output node.

III. MEASURES

A. Perturbation Spreading

RBNs are typically studied as closed systems in which the notion of damage spreading is used to classify the RBNs' dynamics as ordered, critical, or chaotic [15]. Because our model requires external perturbations, we must extend the notion of damage spreading to account for RBNs which are continuously excited by external input. Since an RBN used as a reservoir is not a closed system, the propagation of external perturbations may behave distinctly from the propagation of damage in the initial states of the RBN. Let $\mathcal{M}$ be an RBN with N nodes and average connectivity $\langle K \rangle$. Let u_a be an input stream, and

input layer   reservoir   readout layer

$I = 1$ $N = 5$ $O = 1$
$L = 2$ $\langle K \rangle = 2$

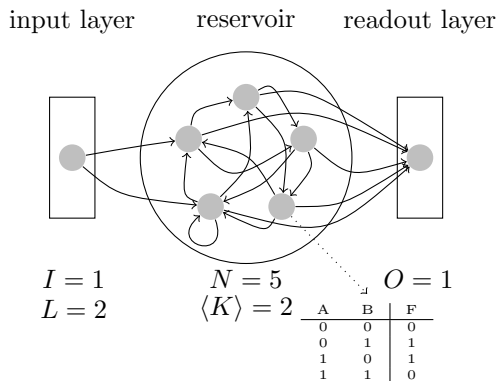| A	B	F
0	0	0
0	1	1
1	0	1
1	1	0

FIG. 1. Schematic of a reservoir computing system. The input layer delivers the input signals to random nodes inside the reservoir. The readout layer receives output signals from random nodes inside the reservoir. The reservoir itself is made of a collection of computing nodes that are randomly interconnected. The reservoir creates a representation of the input signals that can be read and classified by the readout layer. Learning is performed by training only the readout layer nodes and connections.

u_b be a variation of u_a. Then the perturbance spreading of $\mathcal{M}$ with an input stream u_a and its variation u_b is $\mathcal{P}(\mathcal{M}, u_a, u_b) = \frac{H(A,B)}{N}$, where A and B are the states of the RBN after being driven by input streams u_a and u_b respectively, and $H(A, B)$ is the Hamming distance between the states.

For a dynamical system to act as a reservoir, it needs to be excited in different ways by very different input streams, while eventually forgetting past perturbations. These measurements are captured by the notions of *separation* and *fading memory* in [12]. However, to account for the importance of short-term memory in the reservoir and finite-length input streams, we are specifically interested in the *separation* of the system τ time steps in the past, within an input stream of length $\mathcal{T}$.

The ability of the RBN to separate two input streams of length $\mathcal{T}$, which differ for only the first $\mathcal{T} - \tau$ time steps, is given by

$$\mathcal{S}_\tau(\mathcal{M}, \mathcal{T}) = \mathcal{P}(\mathcal{M}, u, v), \qquad (1)$$

where $\mathcal{T} = |u| = |v|$ and

$$v_i = \begin{cases} \bar{u}_i, & \text{if } i < \mathcal{T} - \tau \\ u_i, & \text{otherwise.} \end{cases}$$

In order for an RC device to be able to generalize, a reservoir needs to eventually forget past perturbations. Thus we define:

$$\mathcal{F}(\mathcal{M}, \mathcal{T}) = \mathcal{P}(\mathcal{M}, u, w), \qquad (2)$$

where $\mathcal{T} = |u| = |w|$ and

$$w_i = \begin{cases} \bar{u}_i, & \text{if } i = 0 \\ u_i, & \text{otherwise.} \end{cases}$$

Natschläger et al. [12] found that computational capability of recurrent neural network reservoirs are greatest when the difference between *separation* and *fading memory* are largest and that this coincides with critical dynamics. Therefore, we want fading memory to be low, while separation is high. We define the computational capability of a reservoir $\mathcal{M}$ over an input stream of length $\mathcal{T}$, τ time steps in the past as:

$$\Delta(\mathcal{M}, \mathcal{T}, \tau) = \mathcal{S}_\tau(\mathcal{M}, \mathcal{T}) - \mathcal{F}(\mathcal{M}, \mathcal{T}). \qquad (3)$$

B. Entropy and Mutual Information

Information theory [16] provides a generic framework for measuring information transfer, noise, and loss between a source and a destination. The fundamental quantity in information theory is Shannon information defined as the entropy $\mathcal{H}_S$ of an information source S. For a source S that takes a state $\{s_i | 1 \leq i \leq n\}$ with probability $p(s_i)$, the entropy is defined as:

$$\mathcal{H}_S = -\sum_{i=1}^{n} p(s_i) \log_2 p(s_i). \qquad (4)$$

This is the amount of information that S contains. To measure how much information is transferred between a source and a destination, we calculate the mutual information $\mathcal{I}(S : D)$ between a source S and a destination D with states d_j. Before we can calculate $\mathcal{I}(S : D)$ we need to calculate a joint entropy of the source and destination as follows:

$$\mathcal{H}_{SD} = -\sum_{i=1}^{n} \sum_{j=1}^{m} p(s_i, d_j) \log_2 p(s_i, d_j). \qquad (5)$$

Now the mutual information is given by:

$$\mathcal{I}(S : D) = \mathcal{H}_S + \mathcal{H}_D - \mathcal{H}_{SD}. \qquad (6)$$

We will see later how we can use entropy and mutual information to see how much information from the input signals are transferred to the reservoir and how much information the reservoir can provide about the output while it is performing computation.

C. Tasks

We use the temporal parity and density classification tasks to test the performance of the reservoir systems. According to the task, the RC system is trained to continuously evaluate n bits which were injected into the reservoir beginning at $\tau + n$ time steps in the past.

1. Temporal Parity

The task determines if n bits $\tau + n$ to τ time steps in the past have an odd number of "1" values. Given an

input stream u, where $|u| = \mathcal{T}$, a delay τ, and a window $n \geq 1$,

$$\mathcal{A}_n(t) = \begin{cases} u(t - \tau), & \text{if } n = 1 \\ \oplus_{i=0}^{n-1} u(t - \tau - i), & \text{otherwise,} \end{cases}$$

where $\tau + n \leq t \leq \mathcal{T} - \tau - n$.

2. Temporal Density

The task determines whether or not an odd number of bits $\tau + n$ to τ time steps in the past have more "1" values than "0." Given an input stream u, where $|u| = \mathcal{T}$, a delay τ, and a window $n = 2k + 1$, where $k \geq 1$,

$$\mathcal{B}_n(t) = \begin{cases} 1, & \text{if } 2\sum_{i=0}^{n-1} u(t - \tau - i) > n \\ 0, & \text{otherwise,} \end{cases}$$

where $\tau + n \leq t \leq \mathcal{T} - \tau - n$.

3. Training and Evaluation

For every system, we randomly generate a training set S_T and testing set S_G. For each stream $v \in S_T$ or $u \in S_G$, $|v| = |u| = \mathcal{T}$. The size of the training and testing sets are dependent on n, and determined by the following table.

n	$|S_T|$	$|S_G|$
1	50	50
3	150	150
5	300	150
7	500	150
9	500	150

We train the output node with a form of stochastic gradient descent in which the weights of the incoming connections are adjusted after every time step in each training example. Given our system and tasks, this form of gradient descent appears to yield better training and testing accuracies than the conventional forms. We use a learning rate $\eta = 0.01$, and train the weights for up to 20,000 epochs. Since the dynamics of the underlying RBN are deterministic and reset after each training stream, we terminate training early if an accuracy of 1.0 is achieved on S_T. The accuracy of an RC device on a stream $v \in S_T$ is determined by the number of times that the output matches the expected output as specified by the task divided by the total number of values in the output stream. The accuracy on each input set is summed together and divided by the total number of input streams in the set to calculate the current training accuracy T. After the weights of the output layer are trained on the input streams in S_T, they remain fixed.
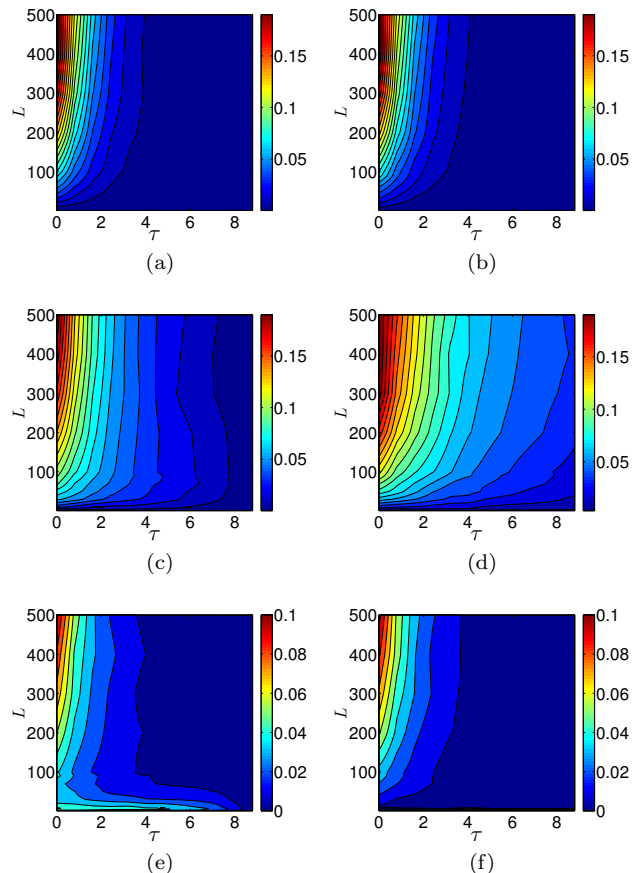

FIG. 2. (Color online) The computational capability Δ of RBN reservoirs with $N = 500$, $L \in [1, N]$ and $\tau \in [1, 9]$. Parameters $\langle K \rangle$ and $\mathcal{T}$ are: $\langle K \rangle = 1$, $\mathcal{T} = 10$ (a), $\langle K \rangle = 1$, $\mathcal{T} = 100$ (b), $\langle K \rangle = 2$, $\mathcal{T} = 10$ (c), $\langle K \rangle = 2$, $\mathcal{T} = 100$ (d), $\langle K \rangle = 3$, $\mathcal{T} = 10$ (e), $\langle K \rangle = 3$, $\mathcal{T} = 100$ (f). The computational capability Δ varies according to $\langle K \rangle \in \{1, 2, 3\}$ and $\mathcal{T} = 10$ in the *left* column and $\mathcal{T} = 100$ in the *right* column.

We then drive the reservoirs with input streams $u \in S_G$ and record the number of times that the output of the RC device matches the expected output. The generalization capability G is then computed by dividing the total number of times in which the output of the readout layer matches the correct output, by the total number of correct outputs. This process is averaged over all streams in S_G. In general, we are interested in finding the reservoirs that maximize G.

IV. RESULTS

A. Computational Capability

The computational capability as predicted by Δ are dependent on the properties of the reservoir $\mathcal{M}$, the length of the input stream $\mathcal{T}$, and the memory τ required by the reservoir. The properties of $\mathcal{M}$ are determined by the dy-
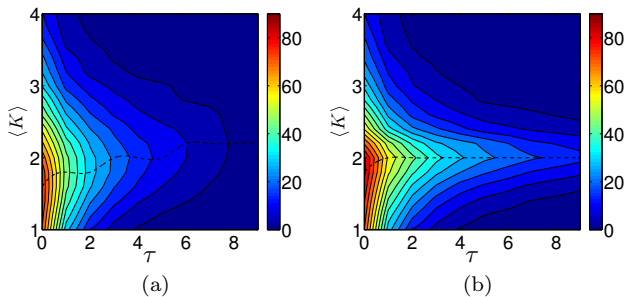
FIG. 3. (Color online) The computational capability Δ of RBN reservoirs $\mathcal{M}$ with $N = 500$ and $\langle K \rangle \in [1, 4]$ summed over $L \in [1, 500]$. These are calculated as: $\sum_{L=1}^{N} \Delta(\mathcal{M}, \mathcal{T}, \tau)$, where $\mathcal{T} = 10$ (a), and $\sum_{L=1}^{N} \Delta(\mathcal{M}, \mathcal{T}, \tau)$, where $\mathcal{T} = 100$ (b). The dashed curve is a spline fit to the highest Δ, illustrating that near-critical connectivity maximizes computational capability, particularly in high $\mathcal{T}$.

namics which are due primarily to $\langle K \rangle$ and the number of nodes L which the input directly perturbs. For each L, $\langle K \rangle$, $\mathcal{T}$, and τ we calculate the average $\Delta(\mathcal{M}, \mathcal{T}, \tau)$ of 50 instantiations of $\mathcal{M}$. In figure 2 we present these results for $\langle K \rangle \in \{1, 2, 3\}$. To produce Fig. 3 we sum over $\Delta(\mathcal{M}, \mathcal{T}, \tau)$ for all L. The dashed curves in Figs. 3(a) and 3(b) are spline fits which highlight the greatest Δ values. In Figs. 2 and 3 we see that RBNs with critical connectivity $\langle K_c \rangle = 2$ tend to provide the highest Δ. A high Δ signifies that the reservoir dynamics have the ability to separate different input streams, while having dynamics which are determined more by recent input, than past input. In contrast, a low Δ signifies either or both of the following: i) the reservoir's dynamics are too frozen to separate different input streams effectively or ii) traces of early perturbations are never forgotten by the reservoir. The consequence of i) is the inability to compute difficult tasks, such as $\mathcal{A}_n$ or those which require long short-term memory. The consequence of ii) is great difficulty in generalizing; if past information which is irrelevant to computing the correct output in the readout layer dominates the dynamics of the reservoir, the output layer will be unable to classify the dynamics caused by the more relevant, recent input.

We see that $\langle K \rangle = 1$ has a very high Δ only when τ is small. This is due to the brief short-memory afforded to an RBN with subcritical dynamics. Since a network with $\langle K \rangle = 1$ has little short-term memory, its computational capabilities are unaffected by an increase in $\mathcal{T}$, as demonstrated in Figs. 2(a) and 2(b): there is no memory at all of early perturbations.

Chaotic reservoirs, represented here by $\langle K \rangle = 3$, are characterized by their sensitivity to initial perturbations, and a high *separation*. In two identical, chaotic systems, a single bit difference in their respective input streams will eventually become magnified until the two systems differ by the states of some P nodes. If the initial perturbation is larger than P, then the differences in the

systems will diminish until reaching P. Because of this, a chaotic system could maximize its Δ in two different ways: i) compute over a sufficiently short input stream and ii) perturb enough of the system so that the recent input has a more significant effect on the dynamics than the past input. In i), the restriction of a brief input stream can be relaxed if the input stream perturbs as few nodes as possible, giving the system more time to propagate perturbations (cf. Fig. 2(e)). On the other hand ii) requires maximizing L (cf. Fig. 2(f)). However, even if distortion is staved off by slowing down the propagation of external perturbations, the system is ultimately fated to disorder.

B. Information and Optimal Perturbation

In the traditional implementations of reservoir computing, all the nodes in the reservoir are connected to the source of the input signal. Many task specific and generic measures of computation in reservoirs have been comprehensively studied in [13]. However, the relationship between the computational properties of the reservoir and the number of nodes which the input layer perturbs remains unexplored. Here, we use information theory to characterize the computation in the reservoir as information transfer between the input and the reservoir and between the reservoir and the output.

In reservoir computing, the reservoir is a dynamical system and therefore has intrinsic entropy. The input is also time-varying and we can calculate its entropy. In order to reconstruct the desired function, the output layer has to pick up the traces of the input in the reservoir dynamics. This fact is reflected in the entropy change of the reservoir due to its input and therefore can be measured using mutual information between the input I and the reservoir R, i.e., $\mathcal{I}(I : R)$. In our study we distribute the input to the reservoir only sparsely, we would thus like to find how $\mathcal{I}(I : R)$ changes as a function of L and if there is an optimal L. Moreover we would like to know, given a task to be solved, how much information the reservoir can provide to the output. That is, given the desired output, can the reservoir state be predictive of the output? This is equivalent to determining how much information is transferred from the reservoir to the desired output. We show this measure using $\mathcal{I}(R : O)$ where O indicates the output as the target.

In order to calculate $\mathcal{I}(I : R)$ and $\mathcal{I}(R : O)$, we consider the instantaneous states of the reservoir and its output to calculate the entropy. For the input, we need to calculate the entropy over the states that the input can take over the window size n. For example, on a input stream of length $\mathcal{T} = 50$ bits, window size n, and time delay $\tau = 1$, the input pattern $u_{t_1}^n$ is an n-bit long moving window over the stream, starting at time step $t_1 = 0$, i.e., $\{u_{t_1}^n | 0 \leq t_1 \leq \mathcal{T} - \tau - n\}$. To calculate the entropy of the reservoir we consider the collection of instantaneous reservoir states s_{t_2} at time step t_2, i.e.,

$\{s_{t_2}|\tau + n \le t_2 \le \mathcal{T}\}$. The output pattern is calculated using the output of the $\mathcal{B}_n(t)$ task. A subtlety arises while calculating the reservoir entropy; since the reservoir follows deterministic dynamics, if $L = 0$, where the input signals does not perturb the reservoir, then the reservoir dynamics will be identical when one repeats the experiment. For reservoirs with chaotic dynamics, where each s_{t_2} is unique, we have a many-to-one mapping between the reservoir states and the output patterns and therefore the reservoir states appear to be capable of reconstructing the output completely. To get the correct result, one must calculate the entropy over many streams. In this case, since the corresponding output patterns change every time, the mapping between the reservoir state and the output will not appear predictive of the output. We feed the reservoir with 50 randomly chosen input sequences of length 50. The entropies $\mathcal{H}_I$, $\mathcal{H}_R$, and $\mathcal{H}_O$ are calculated using the states the input, the reservoir, and the desired output takes during this 50 time interval. Note there is no need to have an output layer in these experiments and the calculations are independent of training mechanism.

Figure 4 illustrates $\mathcal{I}(I:R)$, and $\mathcal{I}(R:O)$ as a function of L for reservoirs of $\langle K \rangle \in \{1, 2, 3\}$. For comparison, we have also included $\mathcal{H}_I$, $\mathcal{H}_R$, and $\mathcal{H}_O$. In an ideal reservoir in which the reservoir contains all the information from the input $\mathcal{I}(I:R) = \mathcal{H}_I$, and $\mathcal{I}(R:O) = \mathcal{H}_O$, indicating that the reservoir contains the required information to reconstruct the desired output perfectly. For $\langle K \rangle = 1$ we see that growing L increases $\mathcal{I}(I:R)$ and $\mathcal{I}(R:O)$ to a maximum level below the ideal values even for $L = 500$, where all the nodes in the reservoirs are receiving the input. These systems do not have enough capacity to calculate the desired output perfectly. For $\langle K \rangle = 2$, we see that mutual information increases and reaches the ideal level at $L = 20$. In these systems, the sparse connectivity between input and reservoir is enough to provide all the required information about the input to the reservoir. We see that at the same level of L the reservoir dynamics are completely predictive of the output. For $\langle K \rangle = 3$, the intrinsic dynamics of the reservoir are very rich (supercritical dynamics) and the mutual information between the reservoir and output reaches its peak at $L = 5$. In these systems a small perturbation quickly spreads. The reservoir at this perturbation level will have enough information to reconstruct the output.

C. Task Solving

We calculate the generalization capability G of RBN-RC devices with $\langle K \rangle \in \{1, 2, 3\}$, $N = 500$, and $L \in (0, 500]$ on the $\mathcal{B}_n$ and $\mathcal{A}_n$ tasks with random input streams of length $\mathcal{T} \in \{10, 100\}$. For each set of parameters, we instantiate, train, and test 30 RC devices. Figs. 5 and 6 present cubic spline fits to the average of these results. We observe in Figs. 5 and 6 that critical dynamics provide the most robust generalization capa-
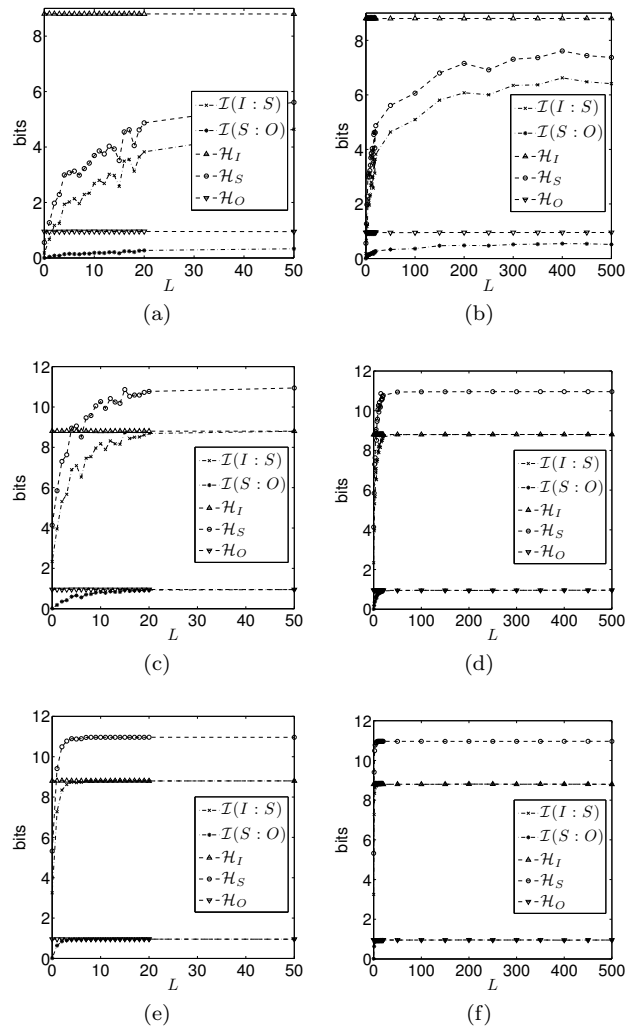

FIG. 4. Mutual information between the input and reservoir $\mathcal{I}(I:R)$ and reservoir and output $\mathcal{I}(R:O)$. The results are for: $\langle K \rangle = 1.0$ (a) and (b), $\langle K \rangle = 2.0$ (c) and (d), $\langle K \rangle = 3.0$ (e) and (f). We have also included the intrinsic information in the input stream, reservoir, and output. For all of these cases $\tau = 1$. In an ideal reservoir $\mathcal{I}(I:R) = \mathcal{H}_I$ and $\mathcal{I}(R:O) = \mathcal{H}_O$. For $\langle K \rangle = 1.0$, as L grows both $\mathcal{I}(I:R)$ and $\mathcal{I}(R:O)$ grow to a maximum level below the ideal level. The reservoir in these systems does not carry enough information for the output layer to solve the task. For $\langle K \rangle = 2.0$, as L grows, the mutual information grows and reaches the sufficient level at $L = 20$. For $\langle K \rangle = 3.0$, mutual information peaks near $L = 5$. Small perturbation from the input provide enough information to the reservoir to reconstruct the desired output.

bility in task solving. Ordered and chaotic reservoirs can evidently solve tasks under certain circumstances. However, the ordered networks are limited by little short-term memory, while the chaotic networks accumulate extraneous information from past perturbations and demonstrate reduced performance as the length of the input stream increases.
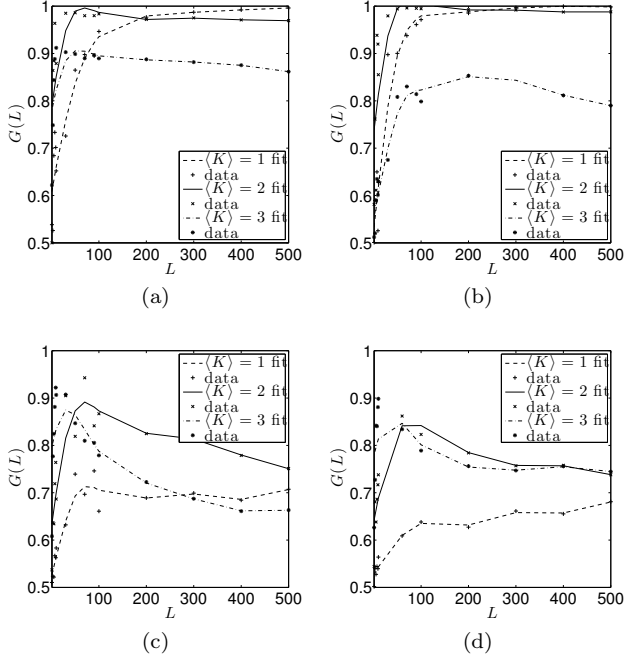
FIG. 5. The generalization capability G of an RBN-RC device $\mathcal{M}$ on the task $\mathcal{B}_n$ is dependent on L and $\langle K \rangle$, as well as task parameters n and $\mathcal{T}$. Here the parameters are: $n = 3, \mathcal{T} = 10$ (a), $n = 3, \mathcal{T} = 100$ (b), $n = 7, \mathcal{T} = 10$ (c), $n = 9, \mathcal{T} = 10$ (d). Notably, chaotic networks achieve their maximum generalization capability with a lower L than ordered networks. Ordered networks possess little memory and so their performance drops as n increases. On the other hand, chaotic networks perform poorly with $\mathcal{T} = 100$ as opposed to $\mathcal{T} = 10$, due to an inadequately fading memory.

1. Average Reservoir Indegree $\langle K \rangle = 1$

When n of $\mathcal{A}_n$ and $\mathcal{B}_n$ is small, there is very little memory and processing required by the reservoir, and so RC devices in which the reservoir has $\langle K \rangle = 1$ can achieve perfect generalization G for $\mathcal{B}_3$ and $\mathcal{A}_3$ (cf. Figs. 5(a) and 6(a)). However, ordered networks are dominated by *fading memory*, hence the dynamics do not retain enough information about past perturbations to achieve high accuracy when n increases. Since the dynamics of ordered networks are only determined by their most recent perturbations, the length of the input stream $\mathcal{T}$ is irrelevant for the task solving capability, which explains why the generalization G of ordered networks computing $\mathcal{B}_3$ is very similar when $\mathcal{T} = 10$ and $\mathcal{T} = 100$, as seen in Figs. 5(a) and 5(b) respectively.

Since memory fades quickly in an ordered reservoir, input cannot propagate swiftly through the network. Moreover, a $\langle K \rangle = 1$ network will almost certainly possess islands. These islands will be unreachable by an input stream that does not strongly perturb the system. In addition, figure 4(b) demonstrates that an ordered network with $\langle K \rangle = 1$ increases its mutual information between input and reservoir $\mathcal{I}(I : R)$ as L increases from 0 to N.
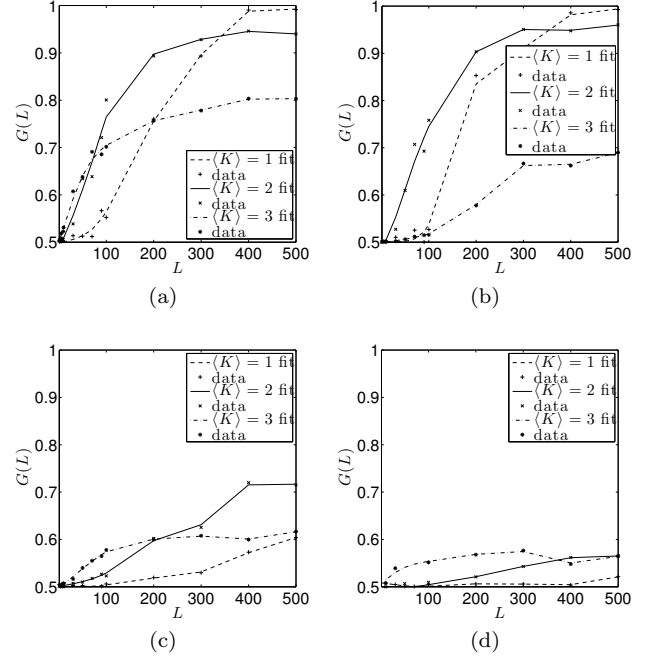

FIG. 6. The generalization capability G of an RBN-RC device $\mathcal{M}$ on the task $\mathcal{A}_n$ is dependent on L and $\langle K \rangle$, and task parameters n and $\mathcal{T}$. Here the parameters are: $n = 3, \mathcal{T} = 10$ (a), $n = 3, \mathcal{T} = 100$ (b), $n = 5, \mathcal{T} = 10$ (c), $n = 7, \mathcal{T} = 10$ (d). Due to high sensitivity to the initial perturbations, the generalization capability of chaotic networks drop as the length of the input stream increases from $\mathcal{T} = 10$ to $\mathcal{T} = 100$. Ordered networks possess little short-term memory and are least robust to an increase in n, with generalization capability on $\mathcal{A}_7$ no better than chance.

Because of this, we see in Figs. 5 and 6 that increasing L tends to result in higher accuracy on $\mathcal{B}_n$ and $\mathcal{A}_n$ respectively. Therefore, an increase of L can only increase the performance of the reservoir.

2. Average Reservoir Indegree $\langle K \rangle = 3$

Chaotic reservoirs, represented here by $\langle K \rangle = 3$, are dominated by the *separation property*. As a result, the G of the chaotic networks are least affected by increasing the window n. However, high performance is only possible when the input stream is sufficiently small, such as $\mathcal{T} = 10$. In Figs. 5(d) and 6(a) the stream length is $\mathcal{T} = 10$ and the G of the chaotic network is high. However, when the length of the input stream is increased to $\mathcal{T} = 100$, the performance drops significantly, even while the performance of networks with lower connectivities remain relatively unchanged (cf. Figs. 5(a) and 5(b)). Though no longer relevant to the RC device, early perturbations have a significant effect on the dynamics, which makes it difficult for the output layer to extract information about the more recent input. On the other hand, if the input stream is sufficiently short, chaotic reservoirs

have less time to be distorted by early input.

In a network which is chaotic due to high connectivity, there will be fewer and larger connected components than in those which are less densely connected [14]. Therefore, the minimal L needed to adequately distribute the input signal in a $\langle K \rangle = 3$ network is less than the other connectivities explored here (cf. Fig. 4(f)). Also, a chaotic reservoir can effectively increase its computational capability as predicted by Δ by reducing its L, which increases the time it takes for perturbations to spread through the system (cf. Fig. 2(e)). Evidently, the chaotic system uses this strategy in computing $\mathcal{B}_n$ when $\mathcal{T} = 10$, as seen in figure 5. However, this behavior is not observed for the highly non-linear parity task $\mathcal{A}_n$. We speculate that, due to the complexity of the task, *separation capability* is more significant than it is in $\mathcal{B}_n$; this causes a strategy which maximizes the *separation property* by increasing L to be optimal.

3. Average Reservoir Indegree $\langle K \rangle = 2$

As observed in figure 3, the difference between the *separation property* and *fading memory* tends to be maximized with near-critical connectivity $\langle K \rangle = 2$. This is evident in our task solving results: when the n of $\mathcal{B}_n$ and $\mathcal{A}_n$ increases, these systems do not show the dramatic drop in G that the ordered systems do (cf. Figs. 5 and 6). Simultaneously, the G of these systems are unaffected by an increase in the stream length $\mathcal{T}$, in contrast to chaotic networks. In figure 4(d) we observe that with $L < 20$ the input signal cannot adequately propagate the input signal, which is demonstrated by a lower G for very small L in Figs. 5 and 6. However, increasing L in task solving appears to afford more of a benefit than simply increasing the information about the input stream. In both Figs. 5 and 6 we see that the best G of the critical networks occurs after the system has already achieved maximal $\mathcal{I}(I : R)$ between input stream and reservoir dynamics.

V. SUMMARY AND DISCUSSION

We investigated the computational capabilities of random Boolean networks when used as the dynamical component in reservoir computing devices. We found that computation tends to be maximized at the critical connectivity $\langle K_c \rangle = 2$. However, in RC, the reservoir is continuously perturbed, and both the size of the perturbations as well as the length of time that the reservoir is perturbed for must be taken into account, along with the chaoticity of the dynamics. If the input stream is sufficiently short, then chaotic systems can still perform quite well, but as the length of the input stream increases, these networks can no longer differentiate and generalize on subsets of the input stream, as the past perturbations, which may no longer be relevant to the computation, are dominating the dynamics. On the other hand, ordered networks can perform well, independent of the length of the input stream, as long as the window of computation is sufficiently small, as an ordered system retains little information about perturbations in the past.

A network view of the RC device can also give us more insight as to why connectivity influences performance. If the reservoir acts on the input stream as a set of spatiotemporal kernels, a suitable reservoir needs to include a diverse set of kernels. In [10], we saw that at the connectivity $\langle K_c \rangle = 2$ the network shows maximal topological diversity and dynamics. A reservoir with connectivity $\langle K_c \rangle = 2$ therefore can act as many networks of the same connectivity, each acting as different kernel.

In [12] and [13] it was shown that optimal computation occurs in recurrent neural networks at the critical points, and our results provide an additional example of this, in a binary, heterogeneous reservoir. In RC, we continuously perturb the reservoir and so the underlying RBN of our model is not a closed system. Therefore, computation cannot be dependent on attractors and must be enabled by the dynamics of the RBN. However, in some circumstances the network dynamics can fall into an attractor temporarily or indefinitely, due to frozen dynamics, inadequate distribution of the input signal, or a non-random input stream. Therefore, RC is a novel framework in which to explore the capacity of RBN dynamics for information processing. RBNs have been studied under other task solving scenarios; in Goudarzi et al. [10] networks evolve towards criticality, although computation is still performed by attractors. Our study shows that unlike the findings in [9], for RBNs there is a strong connection between computation and dynamics, and optimality of the computation is evidently due to critical dynamics in the network. Despite the differences between externally perturbed RBNs in RC and RBNs explored as a closed system, we nevertheless observe that critical RBNs are indeed optimal for reservoir computing. Criticality also plays an important role in biological systems that often require an optimal balance between stability and adaptability. For example, it has been shown by using compelling theoretical and experimental evidence that gene regulatory networks—which are commonly modeled by RBNs—are indeed critical [17, 18].

Our conclusion provides an intriguing link between disparate usages of RBN. By providing evidence that critical dynamics are desirable for heterogeneous substrates in RC, our findings may be relevant to the development of devices which exploit the intrinsic information processing capabilities of heterogeneous, physical systems such as biomolecular or nanoscale device networks.

VI. ACKNOWLEDGMENTS

dergraduate Research & Mentoring Program.

[1] M. Lukosevicius and H. Jaeger, Comput. Sci. Rev. **3**, 127–149 (2009).

[2] C. Fernando and S. Sojakka, ECAL 2003, (Springer-Verlag, Berlin, 2003), LNAI 2801, p. 588–597.

[3] M. Haselman and S. Hauck, Proc. IEEE, **98**, 11–38, (2010).

[4] W. Maass, T. Natschläger, and H. Markram, Neural Comput., **14**, 2531–60, (2002).

[5] H. Jaeger, St. Augustin: German National Research Center for Information Technology Technical Report GMD Rep. 148, (2001).

[6] S. A. Kauffman, J. Theor. Biol. **22**, 437 (1969)

[7] T. Rohlf, N. Gulbahce, and C. Teuscher, Phys. Rev. Lett., **99**, 248701 (2007).

[8] N. H. Packard, in Dynamic Patterns in Complex Systems, ed. by J. A. S. Kelso, A. J. Mandell, and M. F. Shlesinger (World Scientific, Singapore, 1988), p. 293-301.

[9] M. Mitchell, J. P. Crutchfield, and P. T. Hraber, Complex Syst., **7**, 89–130 (1993).

[10] A. Goudarzi, C. Teuscher, N. Gulbahce, and T. Rohlf, Phys. Rev. Lett. **108**, 128702 (2012).

[11] D. Snyder, A. Goudarzi, and C. Teuscher, in Proc. Thirteenth Int'l Conference on the Simulation and Synthesis of Living Systems (ALife 13), (MIT Press, Cambridge, 2012), p. 259–266.

[12] T. Natschläger, N. Bertschinger, and R. Legenstein, in Advances in Neural Information Processing Systems, edited by L. K. Saul, Y. Weiss, and L. Bottou (MIT Press, Cambridge, 2004), **17**, p. 147–152.

[13] L. Büsing, B. Schrauwen, and R. Legenstein, Neural Comput., **22** 1272–1311, (2010).

[14] P. Erdös and A. Rényi *Publ. Math. Debrecen*, **6**, 290–297, (1959).

[15] B. Derrida and Y. Pomeau, Europhys. Lett. 1, 45 (1986).

[16] C. E. Shannon, Bell Sys. Tech. J., **27** 379–423, (1948).

[17] P. Rämö, J. Kesseli, and O. Yli-Harja, J. Theor. Biol., **242**, 164–170 (2006).

[18] M. Nyker, N. D. Price, M Aldana, S. A. Ramsey, S. A. Kauffman, L. E. Hood, O. Yli-Harja, and I. Shmulevich, Proc. Natl. Acad. Sci. (USA), **105**, 1897–1900 (2008).